

Design of freeform lens for WLEDs on the fishing boat

Nguyen Thi Phuong Loan¹, Thinh Cong Tran²

¹Faculty of Fundamental 2, Posts and Telecommunications Institute of Technology, Ho Chi Minh City, Vietnam

²Faculty of Electrical and Electronics Engineering, Ton Duc Thang University, Ho Chi Minh City, Vietnam

Article Info

Article history:

Received Dec 18, 2019

Revised Jan 19, 2020

Accepted Feb 24, 2020

Keywords:

Illumination uniformity

Lighting efficiency

Secondary lens

WLEDs

ABSTRACT

In this article, a free secondary lens is designed for an LED fishing/working lamp (LFWL), which is recommended for the purpose of taking the place of a traditional high-intensity discharge (HID) fishing lamp. To serve the lighting needs of fishing and the on-board activities on fishing boats, the innovative LED lamp is proposed. To make the freeform lens in our optics design process, we depended on Gaussian decomposition. In this way, it is easy to approach the targeted light intensity distribution curve (LIDC) of the LFWL lens. The simulated results show that the performance of the LED fishing/working lamps is much better than that of HID fishing lamps for illumination onboard, on the sea-surface, and underwater. Meanwhile, a lighting efficiency of 91% with the power consumption reduction of more than 50% can be achieved when the proposed LED fishing/working lamps are used instead of the HID fishing lamps.

This is an open access article under the [CC BY-SA](https://creativecommons.org/licenses/by-sa/4.0/) license.



Corresponding Author:

Thinh Cong Tran

Faculty of Electrical and Electronics Engineering,

Ton Duc Thang University,

Ho Chi Minh City, Vietnam.

Email: trancongthinh@tdtu.edu.vn

1. INTRODUCTION

In the modern time, when it has been witnessed a constant development in technology applications. In terms of lighting market, LEDs are considered as a potential and powerful light source that can replace the traditional one. The reason for its popularity comes from its excellent features such as high efficiency, long lifetime, fast reaction and environmental friendliness [1-8]. Nevertheless, it is hard to get all the abilities of conventional radiation pattern of LEDs fully employed, so the LEDs packages need support from additional optical devices [9-12]. Therefore, using a secondary freeform lens, which is introduced to convert the raw radiation pattern into a more suitable one, as an additional optical device seems to be the best solution [13-17]. Besides, owing to their freeform surfaces, this kind of lenses can help to generate more uniformity lights and a proper light intensity distribution curve (LIDC) [18-21]. To the best of our knowledge, there has been no function proposed to achieve an ideal LIDC through the use of secondary lenses. Recently, many researchers have concentrated on creating suitable design of light patterns used in fishing. As mentioned in the 2012 study of Shen's group, to catch the attention of fishes, LEDs applied a light pattern with an alternating distribution of brightness and darkness are used as alternatives for traditional lights [22]. This intensity distribution curve was demonstrated by the Taylor series. Two years later, Shen and his partners designed a novel lens having a capability of generating a light pattern of multiple concentric circles for appealing fish shoals by applying Fourier series and an energy mapping method [23]. Based on the Taylor series and Fourier series, the mentioned LIDCs are exhibited in details, and thus it saves a lot of time to calculate and simulate these LIDCs. In addition, the coefficients of the exponential terms and the emitted angle of LED are utilized to present LIDCs applying

Taylor series. Besides, the computation of the LIDCs are carried out based on the sine and cosine functions in Fourier series. Although these series can reduce the amount of time computing and simulating the LIDCs, a detailed presentation of the progress and an exact model of LIDCs are hard to achieve. Realizing this difficulty, this study proposes the Gaussian decomposition [24, 25] to have the LIDCs presented more accurately. Moreover, with the use of a set of many variable parameters, consisting the main lobe's position, the multiplying factors, and the standard deviations, the exact simulation of required LIDCs can be accomplished. The main goal that this research try to fulfill is achieving the lighting purpose for both fishing and on-board operations on fishing boats; and the key approach to the success in both circumstances is the application of a freeform secondary lens with power chip LEDs. During the design process, the Gaussian decomposition was calculated and used to model the proposed LFWL light distribution. In addition to the optical design and computer simulation work, optical experiments are presented to show the advantages of the proposed LFWL.

2. LFWL LENS DESIGN

2.1. Gaussian decomposition method

The LFWL is designed to support for both fishing and on-board activities. Specifically, the development of the LIDC of LFWL lens is used for two zones, one is the central area for fishing and the other is the two side lobes for on-board working, which are illustrated in Figure 1. The lateral lobe zones are set up through the central peak area for the purpose of obtaining multiple uses from the same LED light power. The light generated by the side lobes is provided for on-board work in fishing vessels. Meanwhile, the light in the center peak region is used to attract the fishes under water.

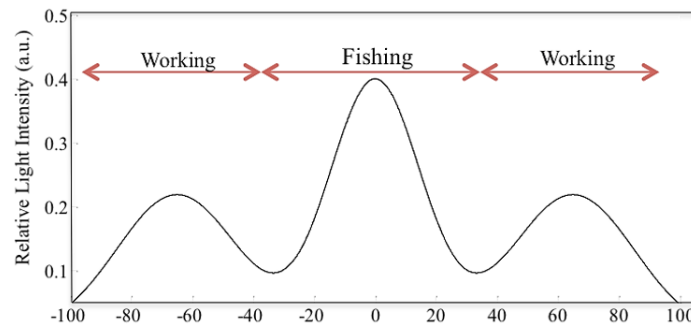


Figure 1. The designed LIDC of LFWL lens

Based on the Gaussian decomposition, the LIDC of LFWL lens can be computed [10, 11] as follows:

$$I_{Lens}(\theta) = \frac{a_0}{\sigma_0 \sqrt{2\pi}} e^{-\frac{\theta^2}{2\sigma_0^2}} + \sum_{n=1}^{\infty} \frac{a_n}{\sigma_n \sqrt{2\pi}} \left(e^{-\frac{(\theta-\mu_n)^2}{2\sigma_n^2}} + e^{-\frac{(\theta+\mu_n)^2}{2\sigma_n^2}} \right) \quad (1)$$

In which μ_0 and μ_n (for $n = 1, 2, \dots$) presents the position of the primary lobe, the n th side lobe, respectively. Meanwhile, the values of multiplying factors a_0, a_1, a_2, \dots and the standard deviations $\sigma_0, \sigma_1, \sigma_2, \dots$ are carefully adjusted to be appropriate to the required LIDC pattern. The values of these parameters corresponding to the desired LIDC pattern are demonstrated in Table 1. Moreover, the workflow of finding the desired parameters by Gaussian decomposition is displayed in Figure 2. The detailed process can be demonstrated as four steps below:

- Step 1: Select the initial key parameters of the Gaussian mixtures based on the idea of the LIDC pattern of the LFWL lens including the number of side lobes, and the position of the main lobe and all side lobes.
- Step 2: Determine the parameter of standard deviations, meaning that determining the width of the main lobe and side lobes based on the design requirement.
- Step 3: Run the minimum mean square error (MMSE) estimation algorithm to find the multiplying factors a_n for $n = 1, 2, \dots$

- Step 4: If the MMSE is within an acceptable region, i.e. $MMSE < \varepsilon$, where $\varepsilon = 10^{-3}$ is the maximum acceptable error, then stop the procedure. Otherwise, go back to Step 2 and adjust the values of σ_n , then repeat the algorithm.

Through the process of design, the LIDC of LFWL lens, which is up to standard, can be appeared by the superposition of Gaussian functions with the proper parameters. These parameters are computed and indicated in Table 1, which results in the analytical solution of the LIDC proposed in Figure 1.

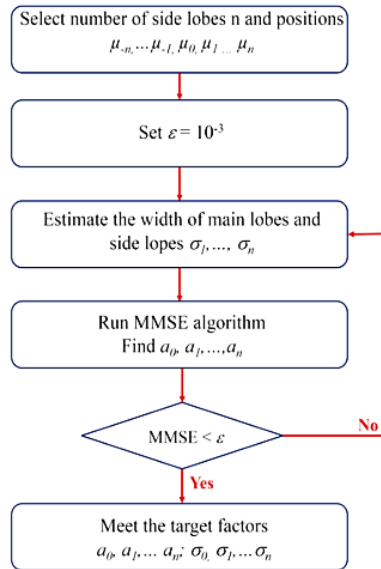


Figure 2. Flow chart of finding the target factor using Gaussian decomposition

Table 1. Designed parameters of the LIDC for LFWL lens using gaussian decomposition

| Design parameters | Values |
|-------------------|--------|
| a0 | 15.04 |
| a1 | 10.98 |
| μ1 | 65 |
| σ0 | 20.35 |
| σ1 | 39.63 |

2.2. Construction of the LFWL lens

The (2) below is use to calculated the normalized luminous intensity distribution curve (LIDC) of the light source. In this formula, each angle is presented by θ , and their luminous intensity is indicated by $I_{LED}(\theta)$.

$$I_{LED}(\theta) = I_a \cos^x(\theta) \tag{2}$$

Additionally, the exponential factor x of (2) can be expressed as: $x = -\ln(2)/\ln(\cos\Phi_{0.5})$, where $\Phi_{0.5}$ represents the light-emitting view-angle of the LED that is described as the angle of which the luminous intensity is half of I_a . With $\Phi_{0.5}$ of 60° , the perfect Lambertian-LED can be obtained. The vector equation of Snell’s Law [12] can be written as:

$$n_o O - n_l I = \sqrt{n_o^2 + n_l^2 + 2n_o n_l O \cdot I} \cdot N \tag{3}$$

here, n_o and n_l indicates the refractive index of reflection and incident ray within the lens, respectively. O shows the refraction unit vector and I means the incident unit vector while N represents the normal vector corresponding to the incident and refraction vectors. In Figure 3 is the method of constructing the main curve of the LFWL lens. The LED source’s central region is placed at the origin of a Cartesian coordinate system. The incident ray $I_i (i = 1, 2)$ from the LED source is aimed to the main curve at the corresponding point R_i for generating the refracted ray O_i . The points Q_i and R_i separate the main curve of the LFWL lens into four equal

parts. The $Q_0 Q_1$ and $Q_1 Q_2$ curves are presented by $f_1(x)$ and $f_2(x)$ functions, respectively. The normal vector N_i can be obtained based on the derivation of $f_i(x)$. The end points of the main curve are preset as Q_i , which are the boundary conditions of the (3), combining with the results of $f_i(x)$ derivation. Indeed, the $Q_0 Q_1$ and $Q_1 Q_2$ curves can be obtained by employing angular energy mapping between the LIDC of the lens (1) and the LIDC of the LED source (2), and then substituting the mapping relationship into Snell's Law (3). First, the Zemax optics design program is employed to find $f_i(x)$. Moreover, by changing $f_i(x)$, it is possible to freely adjust N_i until O_1 and O_2 are directed to the desired LIDC of LFWL lens. The original 3-D LFWL lens design is presented in Figure 4 (a).

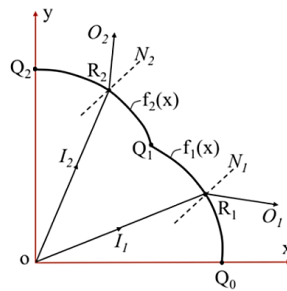
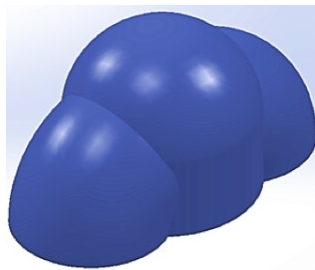
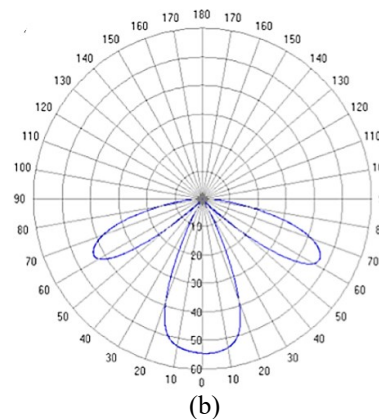


Figure 3. Illustration of 2-D ray-tracing plot of the LFWL lens



(a)



(b)

Figure 4. (a) The 3-D diagrams of the accomplished freeform lens for fishing/working lamp; and (b) it simulated 2-D intensity distribution map

3. RESULTS AND ANALYSIS

In order to successfully get the designing process of the proposed secondary lens under control, we applied Solidworks and the optical design program Zemax to this study. Figure 4 (a) is the illustration of the optimal freeform surface produced by these softwares. The WLED used as a light source for our simulations and experiments is the one having 107 lm luminous flux. Besides, for the best of the fabrication the experimental LFWL module, we attached this white LED package to the optimized freeform lens. Based on the use of Solidworks, the LEDs module is fabricated as a mechanical model, whose key role is as the input to the TracePro program for Monte Carlo ray-tracing carries out the measurement of the light productivity. Displayed in Figure 4 (b) is the simulated 2-D intensity distribution of the proposed LFWL lens. As can be seen, the light generated in the 0~45-degree distribution area is utilized to attract the fishes under water while the light at the distribution zone of 55~85 degrees which is like a pair of bird wings is used for on-board lighting. In Figure 6, the offered LED fishing/working secondary lens is expressed as a specimen, which is suggested for optical experiments.

Moreover, Figure 5 (a) exhibits the material used to create this prototype, which is plastics. Meanwhile, Figure 5 (b) shows the 2-D optical intensity distribution of the LFWL module which is estimated by a goniophotometer. When the LIDCs of LFWL lenses are compared using examples of the two designs: Gaussian decomposition (Figure 1) and the measured LIDC (Figure 6). Next step, to compare the performance

of our proposed freeform lens with the conventional fishing light, the investigation of a 225000 lumens/ 2000 W Philips HID conventional fishing lamp and a 54000 lumens/450 W LED light composed by the array of proposed fishing/working LED modules is carried out. Figure 7 illustrates the measured light distribution curve of the HID fishing lamp.

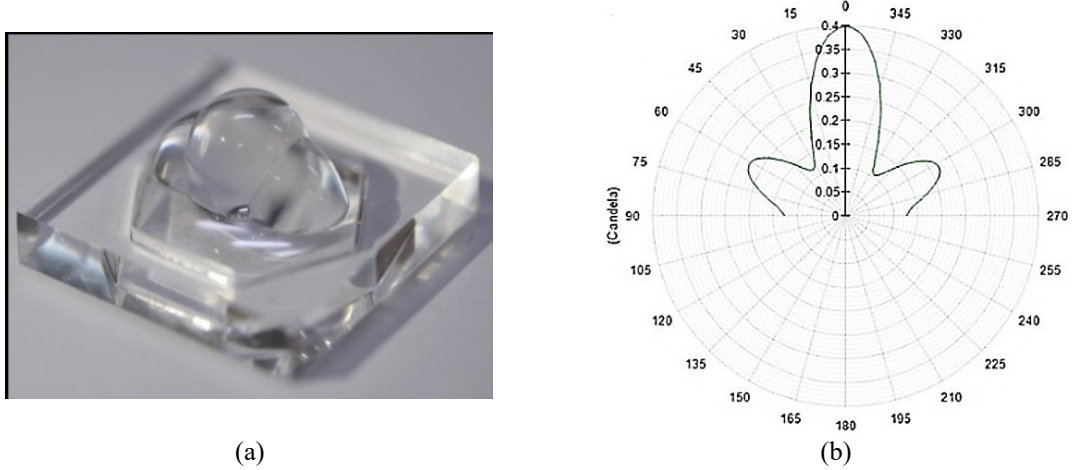


Figure 5. (a) The fabricated freeform lens sample, and (b) its measured 2-D intensity distribution map

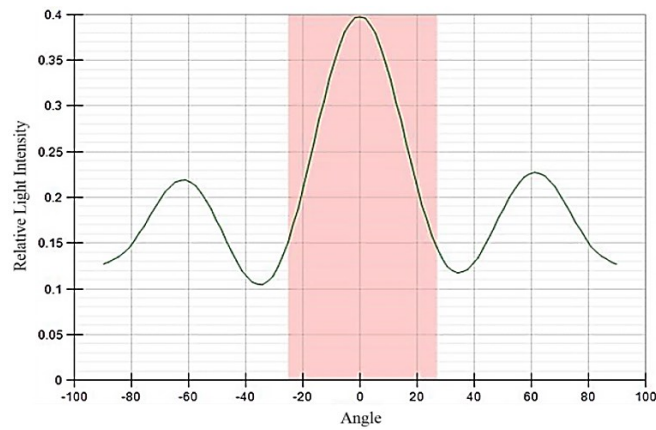


Figure 6. The measured LIDC of LFWL lens

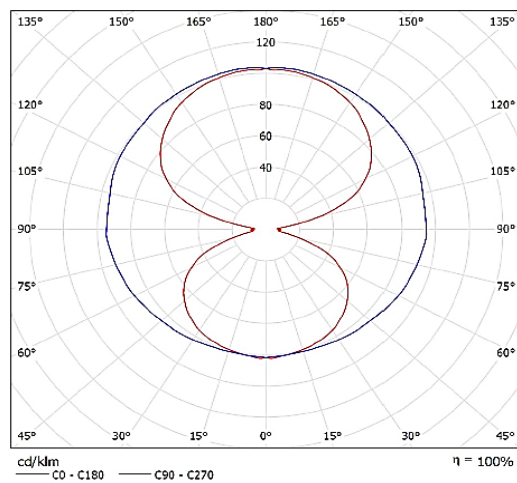


Figure 7. The measured LIDC of the HID fishing lamp

Figure 8 presents the separation between freeform lenses of the LED sets. This separation of 30 mm and 25 mm corresponds to the length and width of the LED set. Then, an examination between the two same sizes 12 m (L) x 3 m (W) fishing boats is conducted. There is a note that the two boats used in our simulation experiments have a board of 2 m higher than the water surface for considering the condition of fishing and working environment. In particular, the first boat is equipped with 30 sets of proposed 450 W LED fishing/working lamps, as illustrated in Figure 9 (a). However, the lighting equipment of the second boat is just 20 sets of the 2000 W HID fishing lamps, as presented in Figure 9 (b). The lamps on two boats are installed on poles, and these poles are located on both sides of the fishing boats with an equal distance from each other, and a height of 2 m from the board floor.

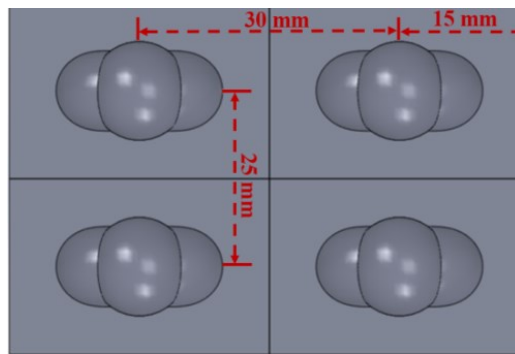


Figure 8. The separations between freeform lenses of the LED sets

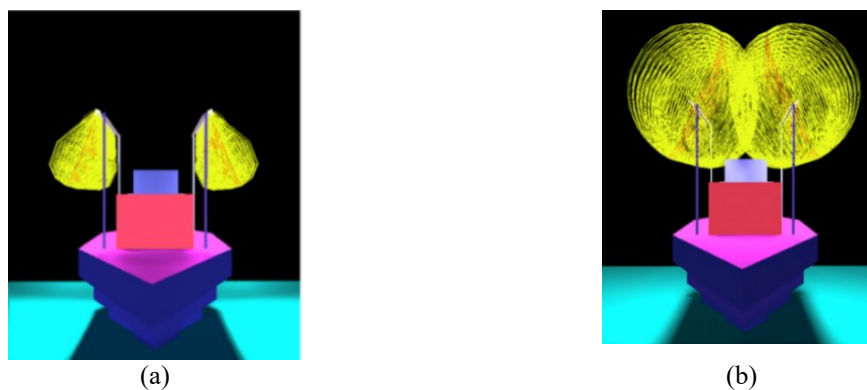


Figure 9. The simulation of the fishing boat equipped with
(a) 30 sets of the 450 W LED fishing/working lamps; (b) 20 sets of the 2000 W HID fishing lamps

In term of evaluating the distribution of light illumination, the DiaLux software is employed to deal with the intensity spreading files (IES file) of the lights, which are obtained by the optical measurements using goniometer. Table 2 is the comparison between the performance of two lighting systems evaluated on different positions: on the board and on the watersurrounding around the fishing vessel. As a result, it is shown that the proposed lamp utilizes just 1/3 the electricity, compared to the traditional HID lamp, but it can bring almost identical illumination distribution regardless of on boat or water. The computation takes account of light absorption of seawater, seawater surface reflectivity, and the light spectrum, then it produces the data of the underwater light illumination distribution at one-meter depth. After analyzing the attained results, we can find that the novel fishing/working LED lamps get 91% efficiency in the seawater transmission, 7% higher than the result of traditional HID fishing lamp (84%). The simulated data of these lamps are all indicated in Table 2.

Table 2. Comparison of the lighting performances between the novel LED fishing lamps and the traditional HID fishing lamps for the fishing boat

| Lamp systems | Power (W) | Board (lux) | Sea-surface (lux) | Underwater (lux) | Efficiency (%) |
|--------------|-----------|-------------|-------------------|------------------|----------------|
| LED lamps | 13500 | 3065 | 1639 | 1315 | 91 |
| HID lamps | 40000 | 2992 | 1768 | 1438 | 84 |

Moreover, the distribution of illumination on the boards is similar in these two cases, as presented in Figure 10. As can be seen in Figure 11, the comparison between the illumination distribution on the sea-surface of two sets of lighting system is clearly displayed. The results imply that both the angle of illumination distribution and the average illumination of the LED sets are smaller than those of the HID sets. However, the deviations are insignificant. Therefore, we can again confirm the efficiency of the proposed LED light and its ability in fish shoals' attractiveness, which brings more benefits than the traditional one.

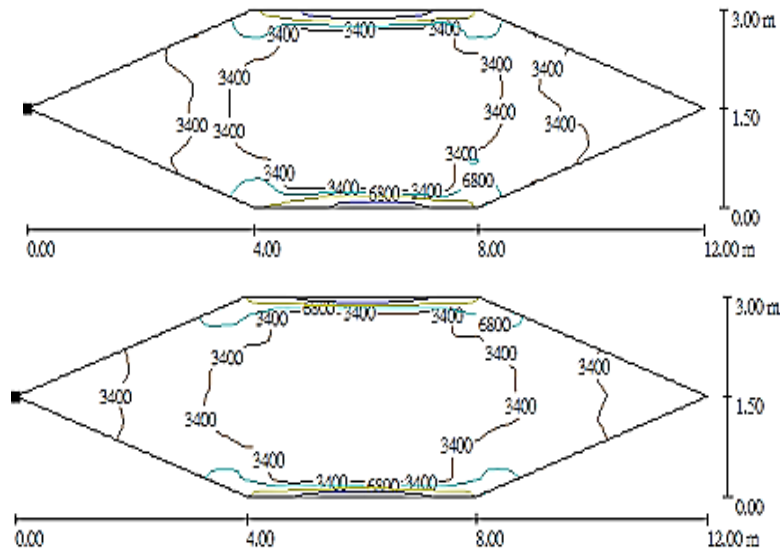


Figure 10. The distribution of illumination on the board of the 30 sets of the 450 W LED fishing/working lamps (top), and the 20 sets of the 2000 W HID fishing lamps (bottom)

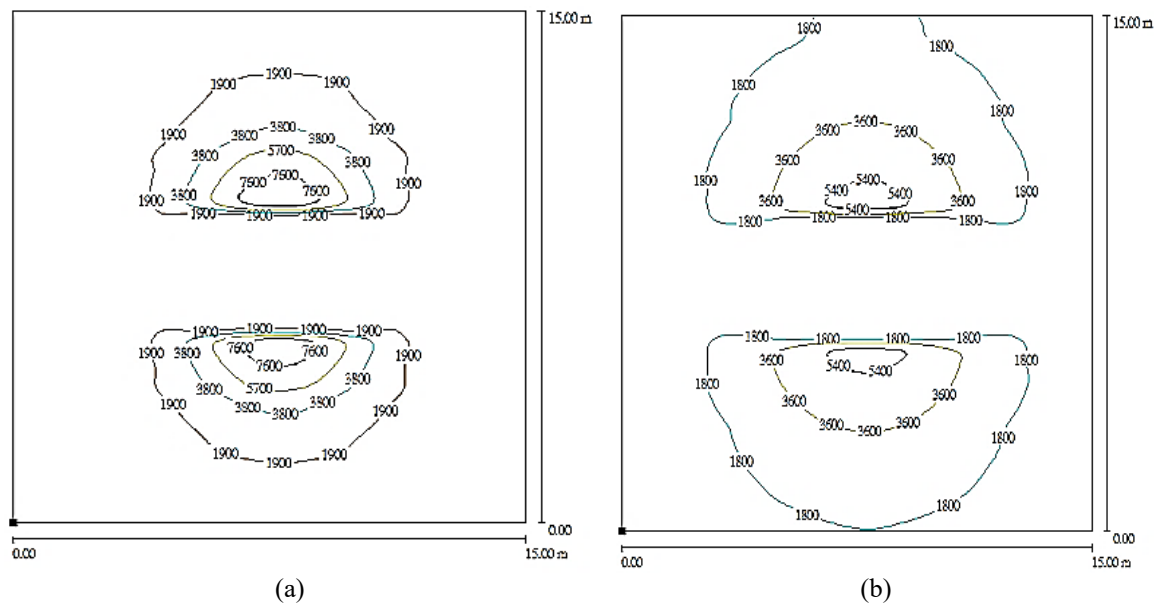


Figure 11. (a) The distribution of illumination on the sea-surface for the 30 sets of the 450 W LED fishing/working lamps and (b) the 20 sets of the 2000 W HID fishing lamps

4. CONCLUSION

This study offers a detailed method for designing a novel freeform lens which serves the purpose of LED fishing/working. The Gaussian decomposition is employed to displayed the LIDC of LFWL lens. Through our experimental results, the traditional HID fishing lamp can be easily replaced by the

fishing/working lamp serving both fishing and on-board working purposes with lower power consumption. Moreover, the simulation results showed that the proposed fishing/working LED lamp can accomplish higher illumination efficiency than the traditional HID lights.

ACKNOWLEDGEMENTS

This research is funded by Department of Science and Technology of Binh Thuan province under grant number DA-02-01-2018.

REFERENCES

- [1] Anh N. D. Q., et al., “Y₂O₃:Eu³⁺ phosphor: A novel solution for an increase in color rendering index of multi-chip white led packages,” *Journal of the Chinese Institute of Engineers*, vol. 40, no. 3, pp. 228-234, 2017.
- [2] Jiang P. G., et al., “Thermally stable multi-color phosphor-in-glass bonded on flip-chip UV-LEDs for chromaticity-tunable WLEDs,” *Applied Optics*, vol. 56, no. 28, pp. 7921-7926, 2017.
- [3] Dinakaran. D., et al., “Phosphor-based light conversion for miniaturized optical tools,” *Applied Optics*, vol. 56, no. 13, pp. 3654-3659, 2017.
- [4] Wang Z., et al., “Single-phase tunable white-light-emitting Sr³La(PO₄)₃:Eu²⁺, Mn²⁺ phosphor for white LEDs,” *Applied Optics*, vol. 56, no. 4, pp. 1167-1172, 2017.
- [5] Xu M. S., et al., “Effects of spectral parameters on the light properties of red-green-blue white light-emitting diodes,” *Applied Optics*, vol. 55, no. 16, pp. 4456-4460, 2016.
- [6] George A. F., et al., “Laser-driven phosphor-converted white light source for solid-state illumination,” *Applied Optics*, vol. 55, no. 8, pp. 1899-1905, 2016.
- [7] Chen M. Z., et al., “Diffractive optical element with same diffraction pattern for multicolor light-emitting diodes,” *Applied Optics*, vol. 55, no. 1, pp. 159-164, 2016.
- [8] Segawa H., and Hirosaki N., “Europium-doped SiAlON and borosilicate glass composites for white light-emitting diode,” *Applied Optics*, vol. 54, no. 29, pp. 8727-8730, 2015.
- [9] Bi W. G., et al., “Improved efficacy of warm-white light-emitting diode luminaires,” *Applied Optics*, vol. 54, no. 6, pp. 1320-1325, 2015.
- [10] Sun W. S., et al., “Simulation and comparison of the illuminance, uniformity, and efficiency of different forms of lighting used in basketball court illumination,” *Applied Optics*, vol. 53, no. 29, pp. H186-H194, 2014.
- [11] Lee H., et al., “Phosphor-in-glass with Nd-doped glass for a white LED with a wide color gamut,” *Optics Letters*, vol. 43, no. 4, pp. 627-630, 2018.
- [12] Anh N. D. Q., and Lee H. Y., “Improving the angular color uniformity and the lumen output for white LED lamps by Green Ce_{0.67}Tb_{0.33}MgAl₁₁O₁₉:Ce,Tb Phosphor,” *Journal of the Chinese Institute of Engineers*, vol. 39, no. 7, pp. 871-875, 2016.
- [13] Myoung S. J., et al., “Material properties of the Ce³⁺-doped garnet phosphor for a white LED application,” *Journal of Information Display*, vol. 17, no. 3, pp. 117-123, 2016.
- [14] Katja M. R., et al., “White LED compared with other light sources: Age-dependent photobiological effects and parameters for evaluation,” *Int. J. of Occupational Safety and Ergonomics*, vol. 21, no. 3, pp. 391-398, 2015.
- [15] Zhuang Z. F., Surman P., and Yu F. H., “A freeform optics design with limited data for extended LED light sources,” *Journal of Modern Optics*, vol. 63, no. 21, pp. 2151-2158, 2016.
- [16] Pradip Kr. M., and Roy B., “Development of dynamic light controller for variable CCT white LED light source,” *LEUKOS*, vol. 11, no. 4, pp. 209-222, 2015.
- [17] Wu R. M., et al., “Direct three-dimensional design of compact and ultra-efficient freeform lenses for extended light sources,” *Optica*, vol. 3, no. 8, pp. 840-843, 2016.
- [18] Sergey V. K., et al., “Development of multiple-surface optical elements for road lighting,” *Optics Express*, vol. 25, no. 4, pp. A23-A35, 2017.
- [19] Lee H. W., and Lin B. S., “Improvement of illumination uniformity for LED flat panel light by using micro-secondary lens array,” *Optics Express*, vol. 20, no. S6, pp. A788-A798, 2012.
- [20] Tomás N., and Arasa J., “Construction method of tailored facets for use in freeform reflectors design,” *LEUKOS*, vol. 11, no. 3, pp. 125-140, 2015.
- [21] Anh N. D. Q., et al., “Design of a free-form lens for LED light with high efficiency and uniform illumination,” *Journal of the Chinese Institute of Engineers*, vol. 53, no. 29, pp. H140-H145, 2014.
- [22] Shen S. C., and Huang H. J., “Design of LED fish lighting attractors using horizontal/vertical LIDC mapping method,” *Optics Express*, vol. 20, no. 24, pp. 26135-26146, 2012.
- [23] Shen S. C., Li J. S., and Huang H. C., “Design a light pattern of multiple concentric circles for LED fishing lamps using fourier series and an energy mapping method,” *Optics Express*, vol. 22, no. 11, pp. 13460-71, 2014.
- [24] Wagner W., et al., “Gaussian decomposition and calibration of a novel small-footprint full-waveform digitising airborne laser scanner,” *ISPRS Journal of Photogrammetry and Remote Sensing*, vol. 60, no. 2, pp. 100-112, 2006.
- [25] Lindner R. R., “Autonomous gaussian decomposition,” *The Astronomical Journal*, vol. 149, no. 138, pp. 1-14, 2015.